Invited Paper

Characteristics of the Stacked Microstructured Solid-State Neutron Detector

S.L. Bellinger*[a], R.G. Fronk[a], W.J. McNeil[a], J.K. Shultis[a], T.J. Sobering[b], D.S. McGregor[a]

[a]S.M.A.R.T. Laboratory, Department of Mechanical and Nuclear Engineering,
Kansas State University, Manhattan, KS 66506

[b]Electronics Design Laboratory,
Kansas State University, Manhattan, KS 66506

ABSTRACT

Silicon diodes with large aspect ratio perforated microstructures backfilled with ^{6}LiF show a dramatic increase in neutron detection efficiency beyond that of conventional thin-film coated planar devices. Described in this work are advancements in the technology with increased microstructure depths and detector stacking methods that work to increase thermal-neutron detection efficiency. Models for ion energy deposition and intrinsic thermal-neutron detection efficiency for the straight trench design are described and results presented. A dual stacked device was fabricated by coupling two detectors back-to-back, along with counting electronics, into a single detector. Experimentally verified results and modeled predictions are compared. The stacked device delivered 37% intrinsic thermal-neutron detection efficiency, lower than the predicted value of 47%. It was determined that this lower observed efficiency is due to detector misalignment in the stacked structure and ballistic deficit from slow charge collection from the deep trench structures. The intrinsic thermal-neutron detection efficiency depends strongly upon the geometry, size, and depth of the perforated microstructures. This work is part of on-going research to develop solid-state semiconductor neutron detectors with high detection efficiencies.

Keywords: solid state neutron detectors, perforated detectors, microstructured semiconductor diode, He-3 replacement technology

1. INTRODUCTION

Coated semiconductor diodes have been studied as neutron detectors for many decades [1], with perhaps the first such device being reported in 1959 [2]. The basic configuration consists of a common Schottky barrier or *pn* junction diode, upon which a neutron reactive coating, such as Gd, ^{10}B or ^{6}LiF, has been applied (see Fig. 1). The advantages of coated diodes as neutron detectors include compact size, a low power requirement, low cost VLSI mass production methodology, and ruggedness. The most commonly used materials used for coated semiconductors are Gd, ^{10}B, ^{6}LiF.

The neutron reactive coating thickness can be optimized by considering the neutron absorption probability, energies and ranges of the reaction products, and the types of ionizing radiation (heavy ions, conversion electrons, gamma rays) [3,13,33]. For ^{6}Li or ^{10}B based coatings, as shown in Fig. 1, thermal-neutron absorption in the neutron reactive coating spontaneously produce two ionizing radiation ions moving in opposite directions; hence only one ion can enter the semiconductor detector volume. Once in the detector volume, the ionizing reaction product loses energy through Coulombic scattering, thereby, creating a charge cloud of electron-hole pairs [3]. An applied voltage causes the excited electron-hole pairs to separate and drift to their respective electrodes, inducing an image charge on the contact electrodes. This charge is integrated and measured by external amplifying and processing electronics, so that the resulting pulse indicates a neutron interaction event. The maximum efficiency is limited by the reaction product ranges, and is no more than 4.5% thermal-neutron detection efficiency [3]. Because basic planar thin-film coated diode detectors have such low thermal-neutron detection efficiencies, they have experienced only modest use as neutron radiation detectors.

* slb3888@ksu.edu; phone 1 785 532-7087; http://www.mne.ksu.edu/research/centers/SMARTlab

Hard X-Ray, Gamma-Ray, and Neutron Detector Physics XII, edited by Arnold Burger, Larry A. Franks, Ralph B. James,
Proc. of SPIE Vol. 7805, 78050N · © 2010 SPIE · CCC code: 0277-786X/10/$18 · doi: 10.1117/12.863603

Downloaded from SPIE Digital Library on 18 Nov 2010 to 129.130.37.22. Terms of Use: http://spiedl.org/terms

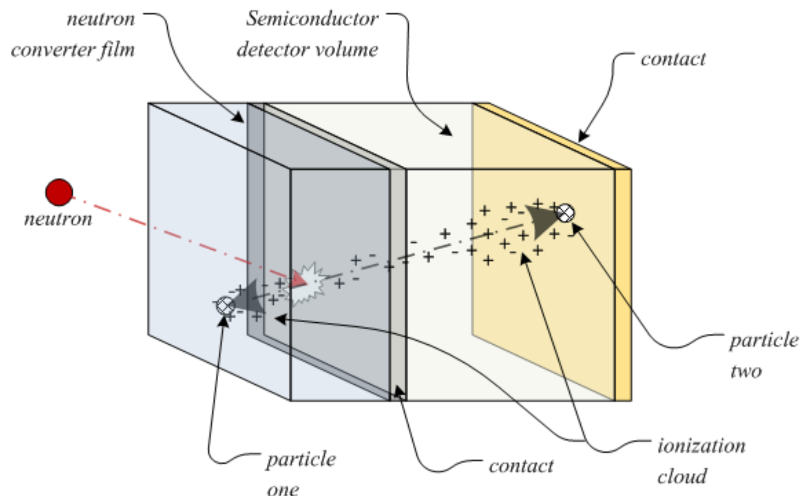

Fig. 1. Basic illustration of the thin-film coated semiconductor neutron detector design. It should be noted that some neutron conversion films produce more than one decay chain, thereby affecting the optimum film thickness. Additionally, notice that due to self-absorption, the film thickness is dictated by the longest reaction product range.

1.1 Neutron reactive coatings

Gadolinium has the highest thermal-neutron cross section of any of the stable nuclides, having two isotopes with large absorption cross sections for thermal-neutrons, those being ^{157}Gd (255,000 b, natural abundance 15.65%) and ^{155}Gd (61,000 b, natural abundance 14.8%). The reactions ^{157}Gd(n,γ)^{158}Gd and ^{157}Gd(n,γ)^{158}Gd lead to the emission of energetic conversion electrons ranging in energy from approximately 29 keV up to 246 keV produced with varying branching ratios [6]. Only 60% of neutron absorptions actually result in the emission of a conversion electron, and of those conversion electrons, 88.5% have energies below 100 keV. Although enriched ^{157}Gd would be preferable, typically natural Gd is used in detectors for economic reasons. The main advantage of Gd as a coating is the large neutron absorption cross section which allows for good neutron absorption with relatively thin films (microns).

The boron isotope ^{10}B (3840 b, 19.9% natural abundance) is commonly used for various neutron detectors, and ^{10}B enriched to over 98% can be acquired for reasonable prices. The ^{10}B(n,α)^{7}Li reaction has two modes of decay, where 94% of thermal-neutron reactions result in the emission of a 1.47 MeV alpha particle and a 840 keV Li ion in the excited state (spontaneously emitting a 480 keV gamma ray), and 6% of thermal-neutron reactions result in the emission of a 1.77 MeV alpha particle and a 1.05 MeV Li ion in the ground state. Boron is a stable material, and in pure form it behaves as a semiconductor (or metalloid) with a resistivity of 10^6 Ω cm, hence detector construction requires the material to be applied in a manner that does not short across rectifying junctions. The main advantage of ^{10}B as a coating over Gd is the emission of higher energy reaction products. Further, the relatively large thermal-neutron absorption cross section yields a macroscopic thermal-neutron cross section of 500 cm^{-1} or an attenuation length of only 20 microns.

The lithium isotope ^{6}Li (941 b, 7.59% natural abundance) is a reactive alkali metal that is used for various neutron absorption and detection purposes. Because of the reactive nature of pure Li, typically the element is used in a stable compound form, such as LiF. The thermal neuron reaction ^{6}Li(n,t)^{4}He releases a 2.73 MeV triton and a 2.05 MeV alpha particle ejected in opposite directions. The reaction products from the ^{6}Li(n,t)^{4}He reaction are more energetic than those of the ^{10}B(n,α)^{7}Li or ^{157}Gd(n,γ)^{158}Gd reactions and, hence, are much easier to detect and discriminate from background radiations. Enriched ^{6}Li, to over 95%, can be acquired for reasonable prices, and the chemical reactions:

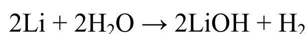

$$2Li + 2H_2O \rightarrow 2LiOH + H_2$$

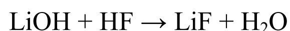

$$LiOH + HF \rightarrow LiF + H_2O$$

are easily used to produce ^{6}LiF in the laboratory environment. The main advantage of ^{6}LiF as a coating over Gd and ^{10}B is the emission of significantly higher energy reaction products, allowing for improved gamma-ray discrimination.

Downloaded from SPIE Digital Library on 18 Nov 2010 to 129.130.37.22. Terms of Use: http://spiedl.org/terms

Although the thermal-neutron absorption cross section for ^{6}Li is large, LiF has a macroscopic thermal-neutron absorption cross section of 57.5 cm^{-1}, which yields an attenuation length of 174 microns, indicating that much thicker films are needed for good efficiency than are required with Gd or ^{10}B.

1.2 The microstructured neutron detector

It was suggested by Muminov et alii that the incorporation of channels in a semiconductor subsequently backfilled with a neutron reactive material could increase the thermal-neutron detection efficiency of a coated diode detector [4], and more recently by Schelten [5,6], Allier [7] and McGregor [8,9,10,11], with much investigative work completed in the last decade [12-38]. Muminov reported that the extended surface area where the neutron reactive material contacted the semiconductor could serve to increase the neutron detection efficiency, which is only partly true. As pointed out later, it is actually the combined effects of the extended surface and the increased probability that reaction products enter the semiconductor, due to geometric effects, that increases the efficiency [12,13,33].

The first demonstration of a microstructured semiconductor neutron detector was reported by McGregor et alii [8,9]. These first detectors were constructed from bulk SI GaAs Schottky diodes with microscopic circular holes, each approximately 4 microns in diameter and 5 microns deep, backfilled with ^{10}B [8,9]. Although showing only a modest increase in efficiency over planar coated semiconductor detectors, these microstructured GaAs detectors proved the validity of the concept. Detectors fabricated from GaAs used the advantageous "truncated field effect" [39], thereby needing only a few volts to operate; hence, the detectors were easily produced, provided that the etched microstructures remained shallow. However, GaAs has higher gamma-ray interaction coefficients than Si, and consequently background gamma-ray interactions will cause lower n/γ discrimination ratios than Si-based detectors. For this reason, and because of the maturity of Si device processing technology, later generations of microstructured detectors were fabricated from Si. The design concept and devices profiles are shown in Fig.2.

Various microstructured device designs, which included circular hole designs (circular, hexagonal), variations of trenches (straight, chevron, sinusoidal), and columns (or pillars) were analyzed for gamma-ray discrimination and efficiency [13,33]. The "hole" microstructure design had the highest gamma-ray discrimination efficiency, but had the lowest thermal-neutron detection efficiency. The columnar or "pillar" design showed the lowest gamma-ray discrimination efficiency, while achieving adequate thermal-neutron detection efficiency. Of these cases, the single-sided design using trench structures provided the highest efficiency while retaining good gamma-ray discrimination.

Microstructured neutron detectors are fabricated by etching microstructured patterns into a semiconductor diode and then backfilling with a neutron conversion material such as ^{10}B or ^{6}LiF. The energetic reaction products in the form of charged particles can be captured within the silicon diode, thereby recording a neutron interaction. These deep microstructures, backfilled with neutron reactive material, increase the neutron absorption efficiency by increasing the probability of registering an interaction.

Inductively-coupled-plasma reactive-ion-etching (ICP-RIE) using high-aspect ratio deep etching (HARDE) techniques, along with common MEMS wet-etching techniques [40,41], are used to fabricate the etched features. Wet-etched straight trench microstructured diode devices (250 microns in depth) have been fabricated and backfilled with ^{6}LiF neutron absorber material (Fig. 2). Two diode variations of the detectors have been fabricated, those being diodes with the rectifying *pn* junction selectively formed around the etched microstructures or with the *pn* junctions conformally diffused inside the microstructures [34,35]. Conformal diffused devices have shown improved performance with more uniform electric fields in the detector active region [25,34,35].

Although the first microstructured devices were fabricated with ^{10}B as the converter [8,9], calculations indicate that higher efficiencies and higher n/γ discrimination ratios are achieved with ^{6}LiF as a converter. Further, because of the higher energies and longer reaction product ranges, the feature dimensions for ^{6}LiF backfilled detectors can be on the order of 10-20 microns, whereas ^{10}B-filled devices must have feature dimensions on the order of 2 microns or less to achieve similar efficiencies. As pointed out elsewhere [23,33], dead-region formation from diffusion and oxidation processes, along with surface damage from the etching processes, compromise efficiency and performance for ^{10}B backfilled devices as opposed to ^{6}LiF devices, mainly because of the smaller features required for ^{10}B backfilled device. ^{10}B has the single advantage that the features need only be 40-60 microns deep to achieve high efficiencies, whereas ^{6}LiF loaded structures must be >250 microns to achieve high efficiency. Because of the numerous advantages, recent microstructured detector fabrication is focused mostly upon ^{6}LiF as the converter [23,29,32,34,35].

Downloaded from SPIE Digital Library on 18 Nov 2010 to 129.130.37.22. Terms of Use: http://spiedl.org/terms

1.3 State of the Art

Although the microstructured neutron detector achieves high thermal-neutron detection efficiency with a single device, designs in which two detectors are stacked, in a staggered fashion, offer the best performance and highest efficiencies. Models of the straight trench detector design, in stacked configuration, were constructed to determine optimum design parameters to achieve the best efficiency while preserving a high n/γ discrimination ratio. A stacked device, in which two microstructured detectors were connected back-to-back into a single detector, was fabricated to demonstrate and test the principle. The intrinsic thermal-neutron detection efficiency for normal incident 0.0253 eV neutrons was measured using a calibrated ^{3}He proportional counter. The neutron response of the stacked detector was also compared to the modeled calculations.

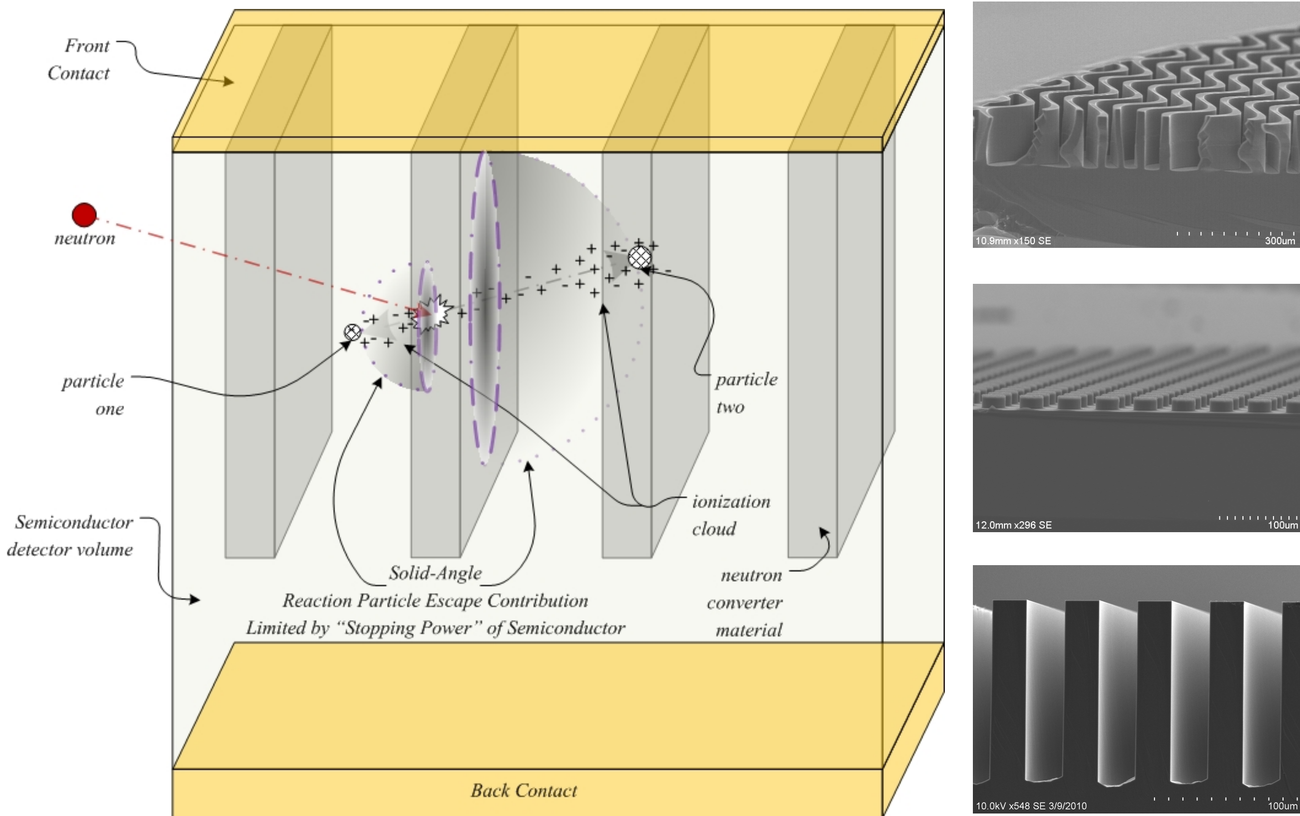

Fig. 2. (Left) Diagram of the microstructured detector concept, showing the reaction product energy deposition tracks through the microstructured semiconductor diode device. (Right) SEM photographs of microstructured Si devices.

2. DETECTOR DESIGN

2.1 Basic Stacked Device Design and Model Geometry

The design studied in the present work consisted of microstructured detectors with straight parallel trenches backfilled with ^{6}LiF (^{6}Li isotopically purified >95%). A detailed discussion on the selection of substrate materials and neutron reactive materials is presented elsewhere [23,33]. Shown in Fig. 3 is the basic stacking concept for the microstructured detectors, in which a second detector is offset from the first detector to prevent neutron streaming through the structure. Note that the 2200 m/s neutron absorption cross section of silicon is small, $\sigma_{Si,a}$ = 0.171 b [42], indicating that the Si substrate does not attenuate neutrons passing through the substrate of the first detector and into the second detector.

Downloaded from SPIE Digital Library on 18 Nov 2010 to 129.130.37.22. Terms of Use: http://spiedl.org/terms

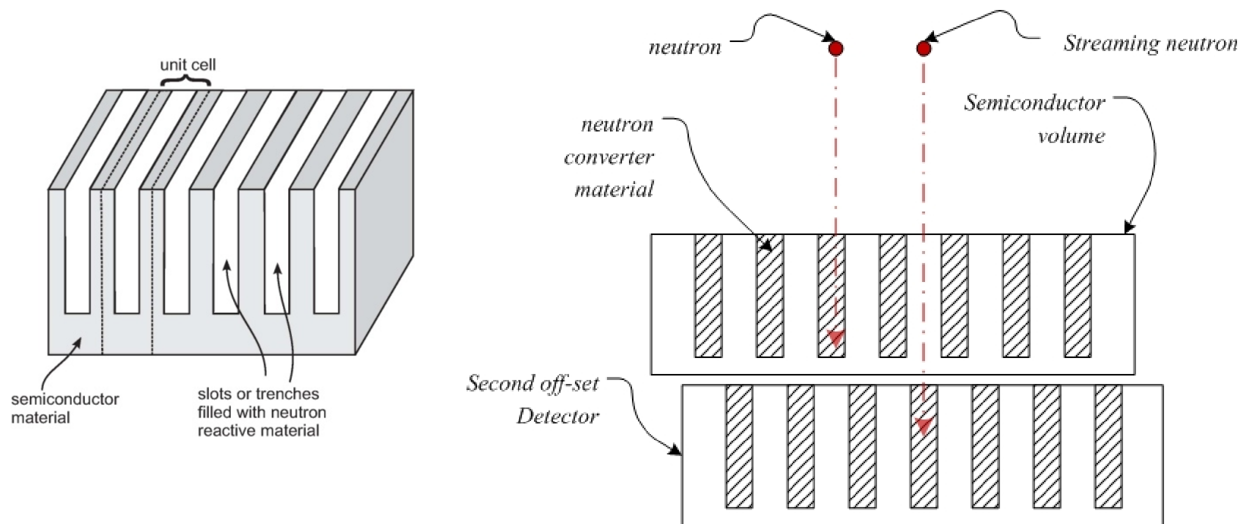

Fig. 3. (Left) The "trench design," composed of etched grooves backfilled with neutron reactive material, showing a unit cell as defined for calculations and modeling. (Right) Neutron detection efficiency is increased, and streaming minimized, by stacking a 2nd detector off-set from the first.

Neutrons that stream through the silicon detection material and are not captured in the neutron reactive material of the first detector, are caught by a second detector if properly arranged off-set from the first detector. Some microstructure patterns are better suited for this stacking arrangement than others. For instance, double stacking of the cylindrical-hole, cylindrical columns (or "pillars"), or hexagonal-hole microstructure patterns do not offer a solution to completely blocking the path of a normally incident parallel beam of neutrons (Fig. 4). A stacked straight trench microstructure pattern can be designed to eliminate neutron streaming through the stacked detectors (Fig. 3).

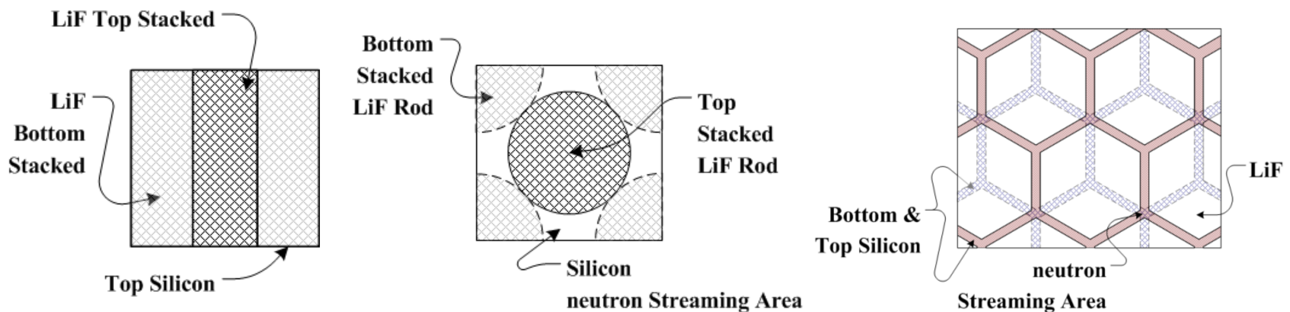

Fig. 4. Stacked detector configurations, showing front and back patterns for the straight trench, circular hole (and pillar), and hexagonal patterns. The stacked trench pattern can be designed with no streaming paths for normally incident neutrons.

2.2 Analytical Approach

To approximate the ion energy-deposition spectra and the corresponding neutron detection efficiencies, some assumptions are used in a Monte Carlo simulation. It was assumed that:

1. The silicon semiconductor was transparent to neutrons and neutron scattering effects were ignored.
2. The detector was irradiated with a parallel beam of thermal-neutrons uniformly and normally illuminating the top surface of the detector.

Downloaded from SPIE Digital Library on 18 Nov 2010 to 129.130.37.22. Terms of Use: http://spiedl.org/terms

3. The neutron absorption cross section for ^{6}LiF converter material is the ion producing cross section (i.e., reactions with F are ignored).
4. All energy deposited in the semiconductor material was assumed to contribute to the pulse height signal of the detector, thereby, ignoring charge transport properties and imperfections in the semiconductor diode.
5. Top and bottom stacked detectors are identical in geometry.

To model the microstructured detector response to thermal-neutrons, a Monte Carlo simulation method was developed, based upon the Shultis-McGregor methodology [23,33], for estimating the ion energy-deposition spectra expected from a single straight trench device design for various dimensions of the etched features. After energy-deposition spectra were developed, the thermal-neutron detection efficiencies were estimated by summing the spectral counts above a specific LLD setting for the various straight-trench device geometries.

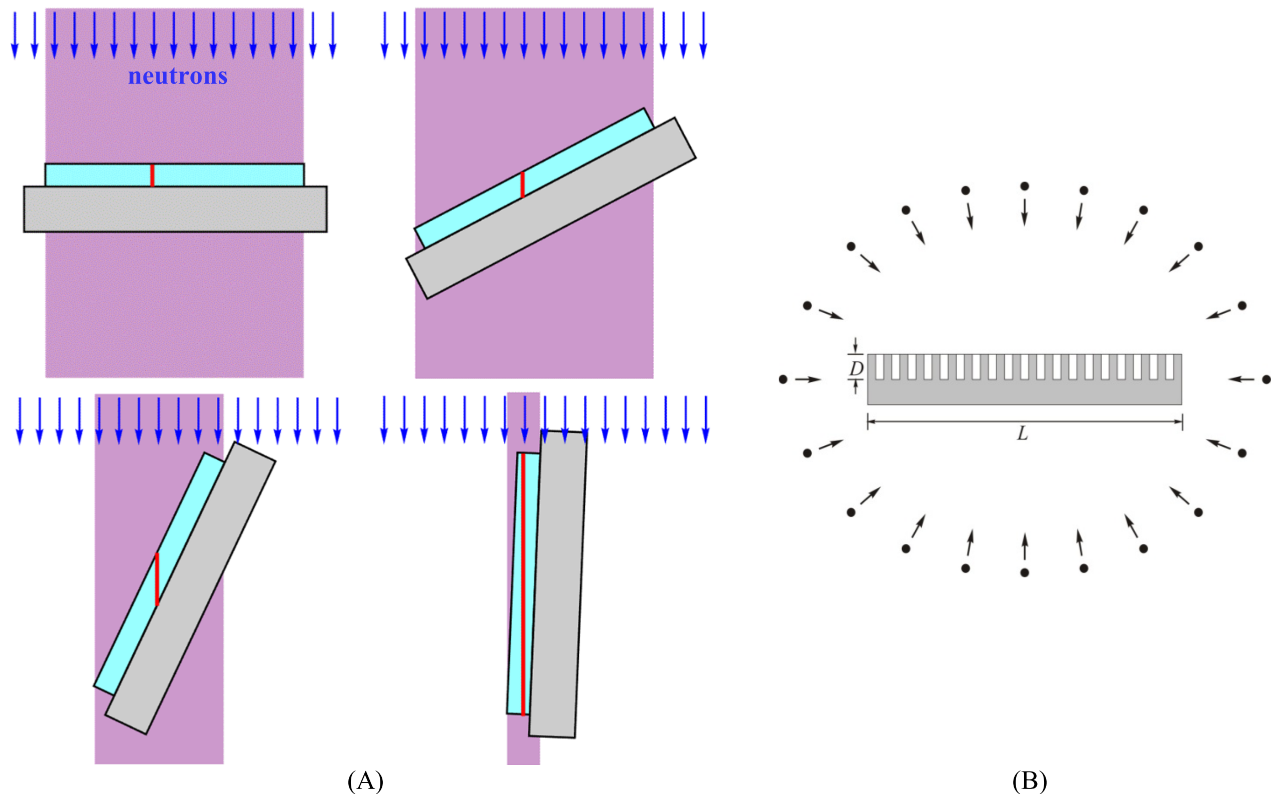

Fig. 5. Shown for (A) is an illustration of the "view factor" (or solid angle) of the detector as the angle changes from normal incidence to nearly zero degree incidence. Although neutron absorption in the reactive film from the side is increased, there is no appreciable detector cross sectional area left for neutrons to intersect. Shown for (B) is an illustration of a center-orientated uniform neutron field configuration. In practical designs, the detector dimensions "L" are much larger than the microstructure depths "D".

2.2.1 Modeled Neutron Beam and Source Considerations

The neutron source was modeled to resemble a diffracted and collimated thermal-neutron beam, available as a standard research tool at numerous research reactor facilities. The thermal-neutron diffraction port at the Kansas State University TRIGA Mark II nuclear reactor was used for the experimental measurements [43], and the diffracted and collimated thermal-neutron beam is well approximated by a parallel beam of uniformly distributed thermal neutrons. Hence, a direct comparison can be made between the experimental performance of the microstructured neutron detectors and that of the modeled thermal-neutron detection efficiencies and ion energy-deposition spectra.

Downloaded from SPIE Digital Library on 18 Nov 2010 to 129.130.37.22. Terms of Use: http://spiedl.org/terms

Note that elsewhere microstructured columnar (or "pillar) devices were modeled using a center-orientated uniform neutron field, with evenly distributed trajectories from 4π-directions [27], a condition that seems difficult to either recreate for verification purposes (except perhaps in the core of a nuclear reactor) or calibrate, which can lead to an incorrect performance assessment. In the parallel beam case that is perpendicular to the device structure, the modeled results give an intrinsic efficiency that can be extrapolated to larger devices. If other neutron angular trajectories are to be considered, then the intrinsic efficiency of the device becomes severely dependent upon the intersection angle (as explained elsewhere [3,16,38]), and a view factor correction must be applied (see Fig. 5). Otherwise, calculations can lead to a severe overestimation of the detector efficiency.

2.2.2 Stacked Detector Simulation Method

The stacked detector arrangement was modeled by calculating and summing the responses of two individual devices. The straight unit cell, as shown in Fig. 3, is a region identical in adjacent cells, and is repeated in the *x* direction. The *y*-direction is considered infinite because the trench length in an actual device is very much larger than the width; hence reaction product energy losses from particles escaping at the ends have little effect on the final result [13,33]. Only a single unit cell is needed to accurately model the expected thermal-neutron detection efficiency. The ^{6}Li(n,t)^{4}He charged particle reaction products exiting the cell at a lateral boundary would be sensed in an adjacent unit cell; hence a reflecting boundary condition for the device was used to include such events.

If the trench and semiconductor "fin" regions are identical in width, a simple exercise of doubling the efficiency would suffice to determine the stacked detector efficiency. However, if the trench is wider than the semiconductor fin, an accounting of absorbed neutrons must be tracked and transferred to the second detector in the stack in order to correctly determine the total neutron interaction rate and thermal-neutron detection efficiency. The stacked detector model included neutron absorption losses from the first detector as they interacted or passed through to the second detector. The neutrons passing through a unit cell of the top detector were recorded, and shifted by half a unit cell to render the neutron interaction rate for a unit cell in the second detector. Afterwards, the reaction product interaction efficiency in the semiconductor was calculated. Fig. 6 shows a neutron transmission image for the top detector, a shifted image of the incident neutron transmission as seen by the bottom detector, and the neutron interaction image for the bottom detector.

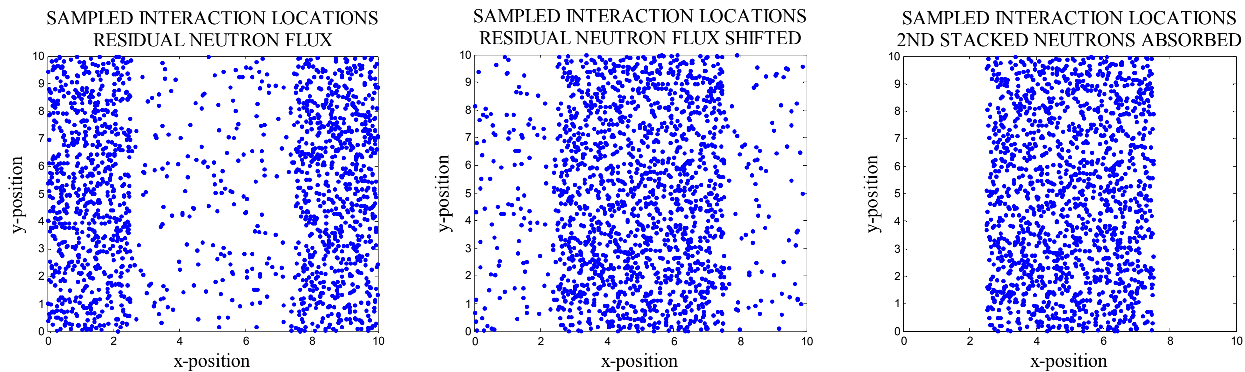

Fig. 6. Show is (left) the neutron transmission image for the top detector where the center portion is the ^{6}LiF-filled trench region, (center) the shifted neutron flux image of neutrons that passed through the top detector so as to align with the bottom detector, and (right) the neutron absorption image for neutrons that interacted in the bottom detector. Note from the left (and center) images that some neutrons passed through the ^{6}LiF material.

If the silicon fin width and ^{6}LiF backfill widths are equal, the device response for the top and bottom detectors are equal. As long as the trench width is greater than or equal to the semiconductor fin microstructure width, the stack configuration will be opaque to neutron streaming. When the trench width is less than the semiconductor fin width, neutron streaming does occur, causing lower neutron detection efficiencies. Fig. 7 illustrates the case where the trench width and semiconductor fin width are not equal, with the ^{6}LiF-filled trench being wider that the semiconductor fin. Although thermal-neutron detection efficiency is increased for the top detector, the thinner semiconductor region absorbs less energy and causes the ion energy-deposition spectrum to shift towards lower energy channels.

Downloaded from SPIE Digital Library on 18 Nov 2010 to 129.130.37.22. Terms of Use: http://spiedl.org/terms

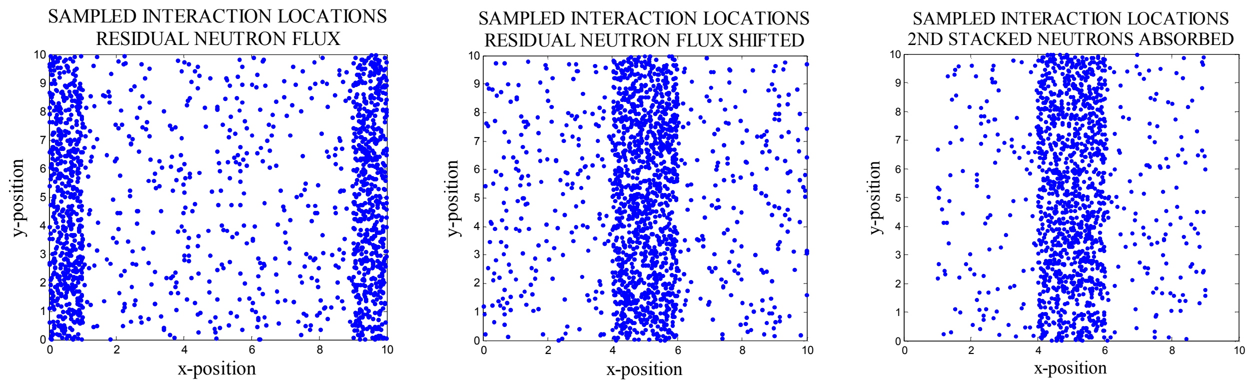

Fig. 7. Shown is a depiction of the neutron flux image transfer operation for a straight trench pattern with the trench width much larger than the semiconductor fin width. Shown is (left) the neutron transmission image for the top detector where the center portion is the ^{6}LiF-filled trench region, (center) the shifted neutron flux image of neutrons that passed through the top detector so as to align with the bottom detector, and (right) the neutron absorption image for neutrons that interacted in the bottom detector. Note from the left (and center) images that some neutrons passed through the ^{6}LiF material. Because the trench is much wider than the semiconductor fin, more neutrons are absorbed in the top detector than the bottom detector.

2.2.3 Modeled Ion Energy-Deposition Spectra for ^{6}LiF Filled Stacked Devices

The stacked straight trench microstructure ion energy-deposition spectra for two varying parameters, depth and trench width, are shown in Fig. 8. Fig. 8(A) and 8(C) show the calculated spectral results for the case in which the ^{6}LiF backfilled region is identical to the semiconductor fin region. Note that the spectral responses for the top and bottom detectors are practically identical, and that the stacked detector efficiency it basically double that determined for a single detector. There are a few notable spectral features, mainly the cut-off energies near 2.0 MeV and 2.7 MeV for the ^{6}Li(n,t)^{4}He reaction products, the total Q value cutoff energy at 4.7 MeV, and the large dip in the energy spectra in the low energy channel region. The large dips in the low energy regions of Fig. 7(A) and 7(C) are fortuitous features characteristic of the microstructure design, caused by the increased probability that one or more reaction products will enter the semiconductor detector with significant energy deposition [23,33]. As a result, the lower level discriminator (LLD) can be set at high values without eliminating many of the neutron counts, thereby, allowing for an increased n/γ discrimination ratio without significantly decreasing the detection efficiency. Fig. 8(B) and 8(D) show the calculated spectral results for the case in which the ^{6}LiF region is much larger than the semiconductor fin region and clearly shows that the top detector has higher efficiency than the bottom detector. Although the total efficiency is greater for the non-symmetric stacked design, it should be noted that the spectral counts have shifted to lower channels and the gap widths of the dip in the spectra have decreased. The efficiency increase is caused by the smaller features of the detector and not the pattern asymmetry. The spectral changes are a consequence of the thinner semiconductor fins, in which less energy is deposited, resulting in more events appearing in the low energy channel regions of the pulse height spectra. The stacked straight trench microstructure devices, in which both detectors have the same microstructure, demonstrate the best ion energy-deposition spectral response of the size parameters considered because of the higher energy response in the spectrum compared to the other microstructure width-parameter designs. Additionally, notice that when the trench depth is 250 microns, few neutrons are actually transmitted through the ^{6}LiF neutron converter material of the top detector. Further discussion of the straight trench ion energy-deposition spectral shape, along with other variant microstructure parameters, is given elsewhere [23,33].

Downloaded from SPIE Digital Library on 18 Nov 2010 to 129.130.37.22. Terms of Use: http://spiedl.org/terms

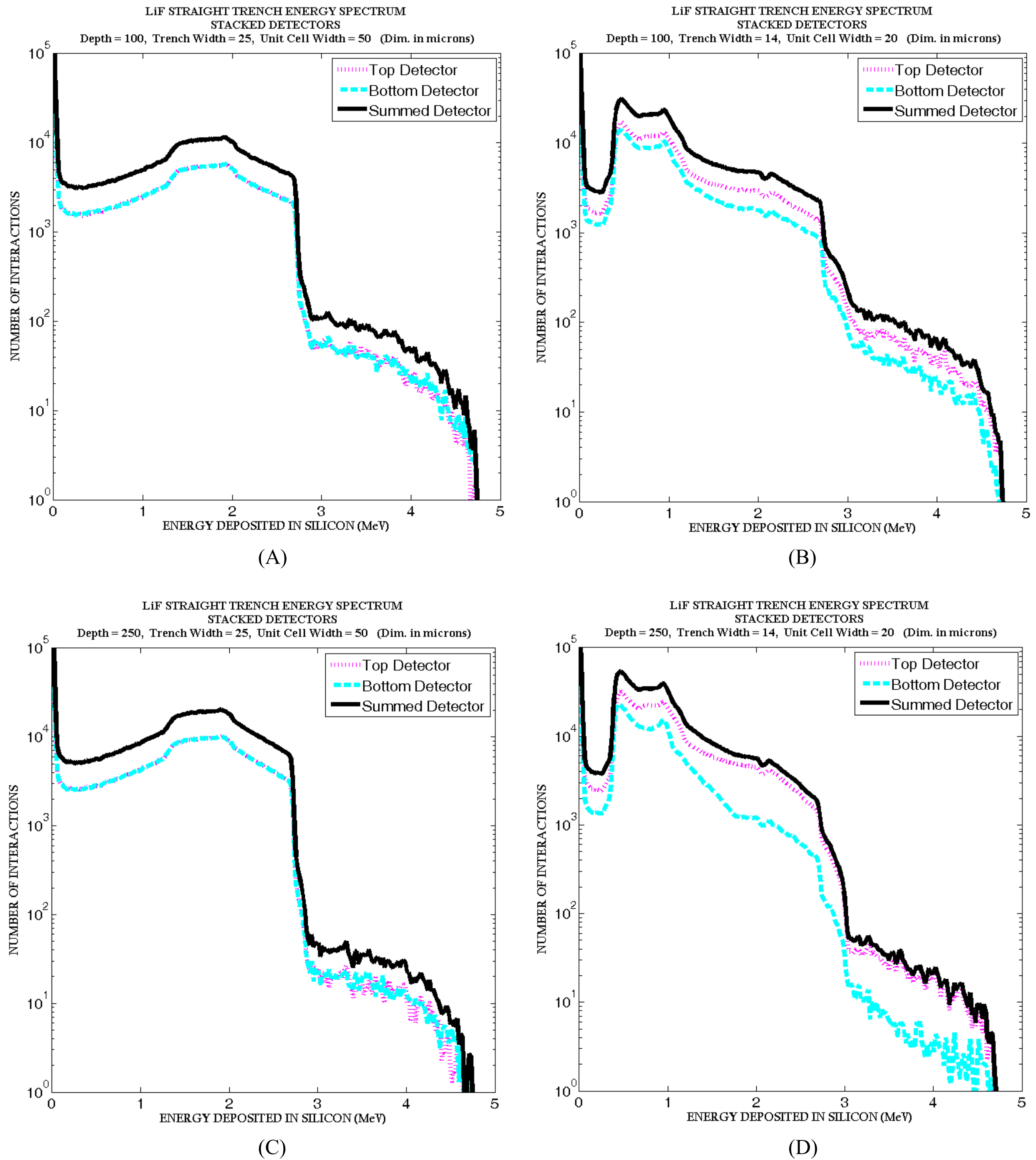

Fig. 8. Straight trench ^{6}LiF-backfilled silicon microstructured stacked detector calculated ion spectra for four cases. Shown in (A) and (C) are cases in which the trenches and semiconductor fins are both 25 microns wide for depths of (A) 100 microns and (C) 250 microns. Shown in (B) and (D) are cases in which the trench and semiconductor fins are unequal, with the trenches being 14 microns wide and the semiconductor fins being 6 microns wide, for depths of (B) 100 microns and (D) 250 microns.

Downloaded from SPIE Digital Library on 18 Nov 2010 to 129.130.37.22. Terms of Use: http://spiedl.org/terms

2.2.4 Modeled Detection Efficiency for ^{6}LiF Filled Stacked Devices

The thermal-neutron detection efficiency of each stacked device design is the fraction of all thermal-neutrons incident on the detector stack that interacts in the converter material and contributes a pulse height signal (ion energy deposition) above a specified LLD setting. Shown in Fig. 9 are the expected intrinsic thermal-neutron detection efficiencies for stacked ^{6}LiF backfilled devices with 250 micron deep features. For non-stacked (single) asymmetric trench structures in which the trench width is wider than the semiconductor fin width produce higher efficiencies than symmetric designs provided that the LLD is set to low energy channels. However, it is the symmetric design that offers higher efficiency for stacked structures.

In most cases, background radiation other than neutrons is present during a measurement, thereby making gamma-ray discrimination important for viable devices. The n/γ ratio increases as the LLD is increased, however valid neutron counts are also eliminated, which consequently lowers the detection efficiency. If the LLD is set in the low energy "dip" region of the spectrum, then only a small fraction of counts are lost and the efficiency is remains high. If the LLD is increased above the "dip" region, then a significant fraction of neutron counts are lost, which lowers efficiency.

From Figs. 8(A) and 8(C), the dip region extends above 1 MeV; hence the efficiency remains high as the LLD is increased up to 1 MeV, as shown in Fig. 9(A). At an LLD setting of 300 keV*, the efficiency for the symmetric case with 25 micron wide, 250 micron deep trenches can deliver a total thermal-neutron detection efficiency of 47%. Note that the decline in efficiency is gradual as the LLD is increased to 1 MeV.

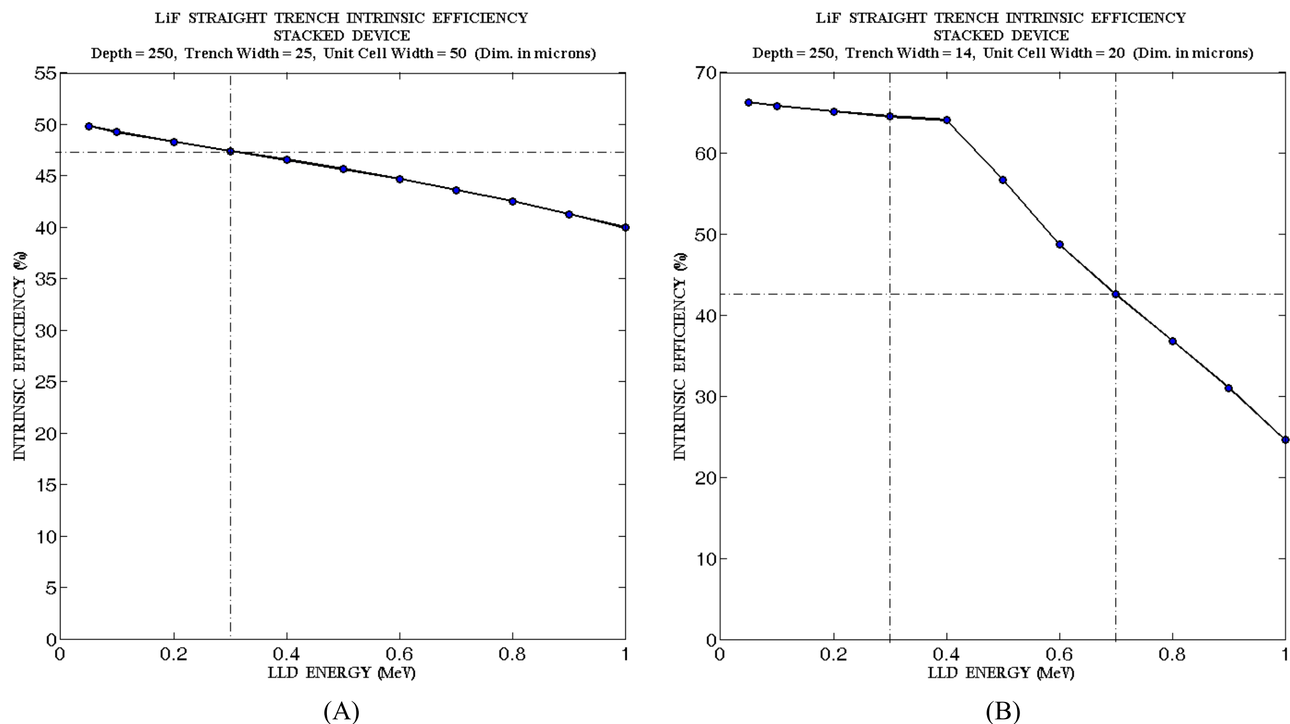

Fig. 9. Predicted ^{6}LiF backfilled straight trench microstructured detector neutron detection efficiencies as a function of the LLD setting for cases in which the cell dimensions are (A) 50 microns with the trench feature size of 25 microns and (B) 20 microns with the trench feature size of 14 microns, with both microstructures 250 microns deep. The observed efficiency from the stacked microstructured devices decreases as the LLD is increased.

The non-symmetric case of Fig. 9(B) with smaller microstructure features clearly has higher efficiencies if the LLD is set in the lower energy regions. However, from Fig. 8(B) and 8(D), the dip in the spectra ends near 400 keV, and

* The LLD setting of 300 keV is five times the crossover energy where Compton scattering becomes dominant over the photoelectric effect in Si.

Downloaded from SPIE Digital Library on 18 Nov 2010 to 129.130.37.22. Terms of Use: http://spiedl.org/terms

setting the LLD above that point will cause significant decrease in efficiency, as shown in Fig. 9(B). Regardless, with the LLD set at 300 keV, the efficiency for the non-symmetric case (14 micron wide trenches, 6 micron wide semiconductor fins) with 250 micron deep trenches can deliver a total thermal-neutron detection efficiency of 64%. Note that the increase in efficiency is directly related to the smaller features sizes and not the asymmetry of the design. Reported elsewhere [33], symmetric trench devices with 10 micron wide trenches and semiconductor fins, yield ~36% intrinsic thermal-neutron detection efficiency at an LLD setting of 300keV. Obviously stacking two of these detectors would exceed the 70% efficiency.

2.3 Discussion

The neutron detection efficiency of the compact microstructured devices can be greatly improved by stacking two offset devices and operating them as a single unit detector. Of all geometries presented here and elsewhere [23, 33], only the trench design and its variants can be stacked such that the front device converter does not shadow the second device converter, while still allowing for the sum of the converter areas to completely fill the total detector area. In other words, the efficiency can be doubled for a trench device. The optimum case for stacked straight trench devices requires that the features be symmetric (trench and semiconductor fin widths are equal). However, if the detector is to be operated as a single device, an asymmetric design where more neutron converter material is present may yield higher efficiencies.

There are non-ideal conditions that will reduce the calculated efficiencies shown in the present work. These conditions include incomplete charge collection, long carrier transport times in the semiconductor that cause ballistic deficit, and leakage currents that increase system noise. Inactive regions, due to mechanical or chemical damage, near the etched surface of the semiconductor will absorb reaction product energy before they reach the semiconductor active region. Collectively, these effects contribute to a spectral shift and ultimately a lower measured efficiency. Yet, the stacked device model can be used to understand expected performance trends and limitations for non-symmetric designs. Future work will concentrate on boron backfilled devices and varying microstructure patterns, including circular hole, pillar, sinusoidal, chevron and hexagonal hole designs.

3. STACKED DETECTOR FABRICATION AND TESTING

3.1 Fabrication Methodology of the Stacked Detector

The detectors were batch processed on (110) 3-inch diameter high resistivity 10 kΩ-cm *n*-type Si wafers. A thick wet oxide was initially grown, through which a diffusion window was patterned. Microstructured perforations were then etched into the Si diffusion windows with an ICP-RIE process or a KOH wet-etch process in which the trench pattern was aligned to the <111> planes in on the (110) orientated Si wafer. Individual detectors were designed with 1 cm^2 active areas. The individual devices had straight trenches etched 250 microns deep by 25 microns wide with a center line pitch of 50 microns. The straight trench design maintains high neutron detection efficiency while creating an opportunity to off-set and stack the detector chips to maximize neutron absorption (as shown in Fig. 2). After the etch process, the wafer was chemically cleaned and *p*-type regions were diffused uniformly into individual device microstructures across the wafer, thereby forming *pn* junctions within the trenches. A Ti-Au metal contact was fabricated on the backside of the wafer to make an electrical ground contact, thereby, completing the diode structure and enabling depletion through the bulk of the individual devices. Finally, ^{6}LiF powder was packed into the perforations to function as the neutron absorbing converter material.

Individual device chips were mounted as a dual-integrated detector system. The dual detector amplifying and readout electronics were designed in-house and consist of a sandwiched detector board and a separate motherboard (see Fig. 10). The separate motherboard configuration was used for research purposes as it simplifies testing multiple detector types through the use of common electronics. On the preamplifier board, a copper foil is sandwiched between two printed circuit boards that have an exposed backside plane. This provides electrical connection for the positive bias voltage. Two neutron detectors were mounted to the copper foil using conductive silver epoxy. On the front of the PC boards the detector anodes were wire-bonded to gold pads that are electrically connected by a post through the sandwiched boards. In this configuration, the anodes of each detector are common and applied to the input of a charge sensitive preamp. A relatively short time constant is used because high counting rates are expected for some applications. The preamplifier board can also be reconfigured such that the feedback from a downstream integrator can be applied to compensate for the large leakage currents that may result from the detector processing steps. All connections to and from the preamplifier board were on a single row 10-pin edge connector. Because the detectors are photosensitive, the stacked

Downloaded from SPIE Digital Library on 18 Nov 2010 to 129.130.37.22. Terms of Use: http://spiedl.org/terms

dual detector and motherboard were placed in a shielded box. Further detail of the stacked device fabrication and electronic readout system can be found elsewhere [37].

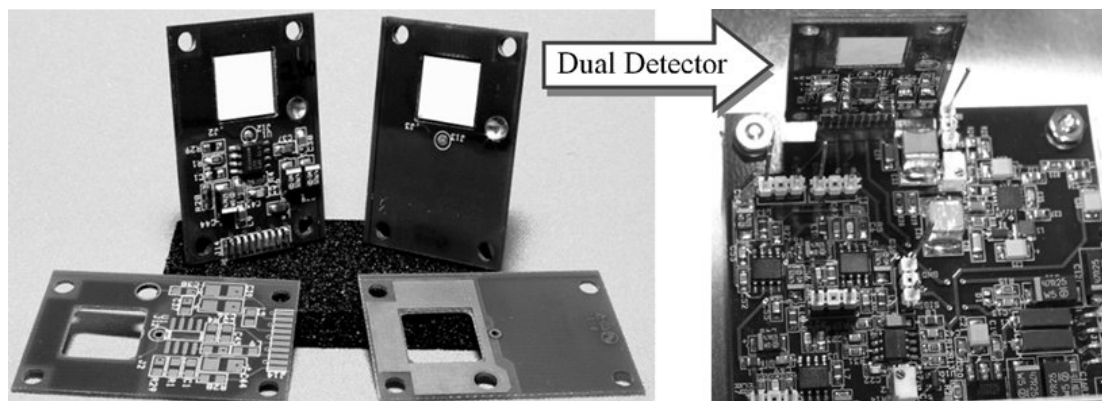

Fig. 10. Shown on the left are dual-integrated packaged devices with preamplifying circuitry. The right picture shows the motherboard, which provides an adjustable detector bias, bias current compensation, pulse shaping and gain, an analog output for pulse-height analysis, and a "digital" output from a discriminator.

3.2 Performance of Stacked Dual-Integrated Neutron Detector

The stacked detector thermal-neutron counting efficiency was measured with a 0.0253 eV diffracted neutron beam from the Kansas State University TRIGA Mark II nuclear reactor. The neutron flux was calibrated with a Reuter-Stokes ^{3}He gas-filled proportional detector and found to be $1.05 \pm 0.02 \times 10^{4}$ cm^{-2} s^{-1}. Details of the calibration method can be found elsewhere [34]. A pulse height spectrum was collected from the stacked dual-integrated microstructured detector in the diffracted neutron beam with and without a beam blocking Cd shutter so as to allow the collection of responses with and without thermal-neutrons. Prompt gamma-rays emitted from the thin Cd shutter appear in the spectrum as numerous pulses at low energy near the noise floor of the detector system (see Fig. 11). The neutron counting efficiency was calculated by dividing the summed neutron counts, collected from the dual detector with a LLD set above the system noise, by the calibrated flux determined with the ^{3}He detector.

Fig. 11 shows the measured pulse height spectrum from the stacked dual-integrated device, reported elsewhere [37], with each detector chip having 250 micron deep trenches. The single dual-integrated device works well with only 2 volts reverse bias. The pulse height spectrum shows many more counts than previously reported for single and dual-integrated devices [29]. Notice that the spectrum shows the expected features, yet these features, including the "dip", appear at lower channels than expected. Some of this shift may be caused by an overall increase in capacitance of the stacked device, thereby, reducing the pulse height signal from the detector, or by a ballistic deficit resulting from slow charge carrier removal from the deep microstructure semiconductor regions. Similar to the other tested devices with the Cd shutter closed [29,34], the gamma-ray component was negligible at a LLD setting above channel 11 (or 375 keV). With the LLD set to channel 11 (375 keV), the intrinsic thermal-neutron detection efficiency was measured to be $37.0 \pm 0.6\%$.

The measured ion energy-deposition spectrum from the stacked dual device does not compare well to the simulated model, although the main features are present. In fact, the spectrum appears to be a closer representation to the stacked device with non-symmetrical features. A device operation simulation was created using the *Silvaco* TCAD software package to understand the effect of the electric fields generated by the conformal diffusion process and the time-response of a signal pulse, whose results and discussion are presented elsewhere [37]. The simulation indicates that the weak electric potential in the silicon fins causes long charge extraction times (> 10 microseconds). With an integration time of only 2 microseconds, ballistic deficit causes the pulse heights to be smaller and shifts the entire energy spectrum to lower channels. Possible solutions to ameliorate these effects include increasing the signal integration time or changing the microstructure diode fabrication process to produce higher electric potential fields within the silicon fins.

Downloaded from SPIE Digital Library on 18 Nov 2010 to 129.130.37.22. Terms of Use: http://spiedl.org/terms

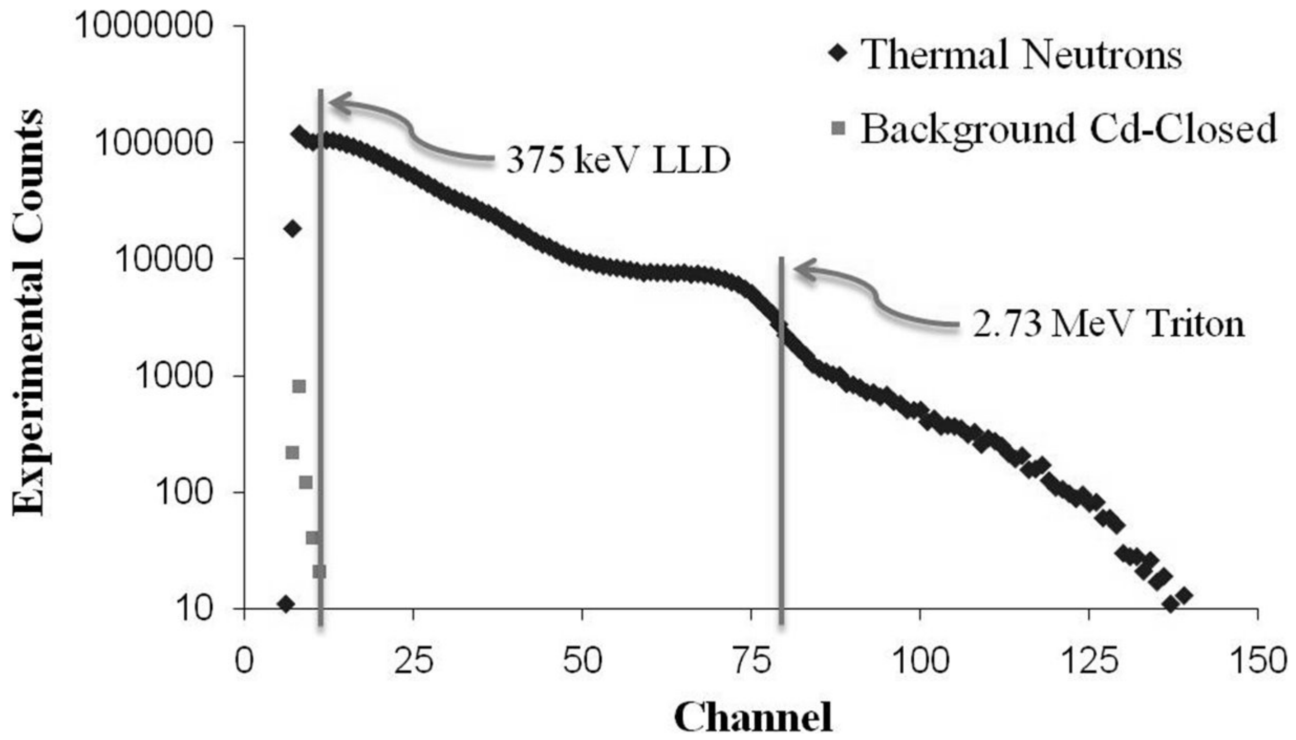

Fig. 11. Pulse height spectrum from conformal-diffused diode dual-integrated detector with 250 micron deep straight trench microstructures, showing responses with and without (Cd shutter closed) neutrons. Electronic signal integration time was 2 microseconds.

3.3 Discussion

The detector design with conformal diffused *pn* junctions within the microstructured trenches has lowered the leakage current and improved the pulse height signal from devices with etched features up to 100 microns deep [25,34]. For detectors with trench depths beyond 100 microns, the pulse height spectra from the stacked dual-integrated detector system are shifted to the low energy channels and do not compare well with the predicted stacked ion energy-deposition spectra modeled earlier. The measured 37% thermal-neutron detection efficiency for the 250 micron deep etched detector was not as high as the 47% predicted by the model. This discrepancy can be explained as follows. First, the bottom stacked device trench alignment may not have been well aligned with the top detector. This has two consequences: neutron streaming can occur for areas not intersected by the converter and the top detector absorber may be shadowing the bottom detector absorber. Overall, the result is a decrease in detection efficiency. Second, the shift may be due to charge collection losses and a ballistic deficit [37]. Future work will be dedicated to better construction, aligning and bonding methods. Also, new fabrication designs of interlaced microstructures, that are etched from both sides of the Si diode, shown elsewhere [11], are being employed. The fabrication design will improve the electric field strength, making it uniformly distributed across the Si detector volume so as to reduce the signal integration time.

Downloaded from SPIE Digital Library on 18 Nov 2010 to 129.130.37.22. Terms of Use: http://spiedl.org/terms

4. CONCLUSION

Based on the results and observations presented here, the following can be stated:

1. Higher efficiency can be achieved by stacking the semiconductor detectors. The efficiencies for symmetric trench devices can be doubled by capturing streaming neutrons from the first detector.

2. The modeled neutron beam characteristics were chosen to closely resemble that of a real world measurement application, thereby, allowing for straightforward model verification and direct comparisons to fabricated devices.

3. With low LLD settings and minimal feature sizes, single devices with asymmetric features (trenches wider than semiconductor fins) offer the highest efficiencies. However, with the LLD set at channels generally necessary to discriminate against background gamma rays, the stacked trench design with symmetric features outperforms the asymmetric designs (stacked or not).

4. A dual-integrated, 1-cm^2 straight trench microstructured Si detector, backfilled with ^{6}LiF powder has been characterized for neutron sensitivity in a diffracted 0.0253 eV thermal-neutron beam from a TRIGA Mark II nuclear reactor. An important advantage for the dual-integrated microstructured neutron detector design is the high efficiency achieved by appropriately stacking two detector chips into a single device. The dual-integrated detector with two 250 micron deep trenched devices achieved 37% intrinsic efficiency. This is below the predicted efficiency of 47% and is likely due to improper stacking alignment and incomplete charge collection.

Stacked dual-integrated trenched microstructured devices, backfilled with ^{6}LiF, offer high thermal-neutron detection efficiency in a compact package. Variants on the trench design have been reported, which include sinusoidal trenches and chevron trenches [29,32,34,35].

5. ACKNOWLEDGEMENTS

This work was supported under DTRA contract DTRA-01-03-C-0051, National Science Foundation IMR-MIP grant No. 0412208, and US Department of Energy NEER Grant DE-FG07-04ID14599.

REFERENCES

[1] *Neutron Detectors*, International Atomic Energy Agency, Bibliographical Series, No. 18, Vienna, 19661966 (references therein).
[2] R.V. Babcock, R.E. Davis, S.L. Ruby, K.H. Sun and E.D. Wolley, "Coated Semiconductor Is Tiny Neutron Detector," Nucleonics, **17**, pp. 116 -122, 1959.
[3] D.S. McGregor, M.D. Hammig, H.K. Gersch, Y-H. Yang, and R.T. Klann, "Design Considerations for Thin Film Coated Semiconductor Thermal-neutron Detectors, Part I: Basics Regarding Alpha Particle Emitting Neutron Reactive Films," Nuclear Instruments and Methods, **A500** (2003) pp. 272 - 308.
[4] R.A. Muminov and L.D. Tsvang, "High Efficiency Semiconductor Thermal-Neutron Detectors," Soviet Atomic Energy, **62**, pp. 255-342, 1987.
[5] J. Schelten, M. Balzhäuser, F. Höngesgberg, R. Engels and R. Reinartz, "A New Neutron Detector Development Based on Silicon Semiconductor and ^{6}LiF Converter," Physica B, **234-236**, pp. 1084-1086, 1997.
[6] J. Schelten and R. Reinartz, Neutron Detector, US Patent 58804762, allowed March 9, 1999.
[7] C.P. Allier, Micromachined Si-well scintillator pixel detectors, DUP Science, The Netherlands, 2001, pp. 132-133.
[8] D.S. McGregor, R.T. Klann, H.K. Gersch, E. Ariesanti, J.D. Sanders, and B. VanDerElzen, "New Surface Morphology for Low Stress Thin-Film-Coated Thermal-neutron Detectors," Conference Record of the IEEE Nuclear Science Symposium, San Diego, California, Nov. 4-9, 2001.
[9] D.S. McGregor, R.T. Klann, H.K. Gersch, E. Ariesanti, J.D. Sanders, and B. VanDerElzen, "New Surface Morphology for Low Stress Thin-Film-Coated Thermal-neutron Detectors," IEEE Trans. Nuclear Science, **NS-49** (2002) pg. 1999-2004.
[10] "Pocked Surface Neutron Detector," D.S. McGregor and R.T. Klann, US-6545281; allowed April 8, 2003.

Downloaded from SPIE Digital Library on 18 Nov 2010 to 129.130.37.22. Terms of Use: http://spiedl.org/terms

[11] "High-Efficiency Neutron Detectors and Methods of Making the Same," D.S. McGregor, R.T. Klann, US-7,164,138; allowed January 16, 2007.
[12] J.K. Shultis and D.S. McGregor, "Efficiencies of Coated and Perforated Semiconductor Neutron Detectors," Conf. Rec. IEEE Nuclear Science Symposium, Rome, Italy, Oct. 18-22, 2004.
[13] J.K. Shultis and D.S. McGregor, "Efficiencies of Coated and Perforated Semiconductor Neutron Detectors," IEEE Trans. Nuclear Science, **NS-53** (2006) pp. 1659-1665.
[14] W.J. McNeil, S. Bellinger, T. Unruh, E. Patterson, A. Egley, D. Bruno, M. Elazegui, A. Streit, D.S. McGregor, "Development of Perforated Si Diodes for Neutron Detection," IEEE Nuclear Science Symposium, San Diego, CA, Oct. 29-Nov. 3, 2006.
[15] D.S. McGregor S. Bellinger, D. Bruno, W.J. McNeil, E. Patterson, B.B. Rice, "Perforated Semiconductor Neutron Detector Modules," Proc. of 32nd Annual GOMACTech Conf., Lake Buena Vista, FL, March 19-22, 2007.
[16] C.J. Solomon, J.K. Shultis, W.J. McNeil, T.C. Unruh, B.B. Rice, and D.S. McGregor, "A Hybrid Method for Coupled Neutron-Ion Transport Calculations for ^{10}B and ^{6}LiF Coated and Perforated Detector Efficiencies," Nucl. Instrum. and Meth., **A580** (2007) pp. 326-330.
[17] D.S. McGregor, S.L. Bellinger, D. Bruno, S. Cowley, M. Elazegui, W.J. McNeil, E. Patterson, B.B. Rice, C.J. Solomon, J.K. Shultis, and T. Unruh, "Perforated Semiconductor Neutron Detector Modules for Detection of Spontaneous Fission Neutrons," IEEE Conference on Technologies for Homeland Security, Woburn, MA, May 16-17, 2007.
[18] Q. Jahan, E. Patterson, B. Rice, W.L. Dunn and D.S. McGregor, "Neutron Dosimeters Employing High-efficiency Perforated Semiconductor Detectors," Nuc. Instrum. and Meth., **B263** (2007) pp. 183-185.
[19] D.S. McGregor, S.L. Bellinger, D. Bruno, W.J. McNeil, E. Patterson, J.K. Shultis, C.J. Solomon, T. Unruh, "Perforated Semiconductor Neutron Detectors for Battery Operated Portable Modules," Proc. SPIE, 6706 (2007) pp. 0N1-0N12.
[20] D.S. McGregor, S.L. Bellinger, D. Bruno, S. Cowley, W.L. Dunn, M. Elazegui, W.J. McNeil, H. Oyenan, E. Patterson, J.K. Shultis, G. Singh, C.J. Solomon, A. Kargar, T. Unruh, "Wireless Neutron and Gamma Ray Detector Modules for Dosimetry and Remote Monitoring," IEEE Nuclear Science Symposium, Waikiki, Hawaii, Oct. 28-Nov. 3, 2007.
[21] S.L. Bellinger, W.J. McNeil, T.C. Unruh, D.S. McGregor, "Angular Response of Perforated Silicon Diode High Efficiency Neutron Detectors," IEEE Nuclear Science Symposium, Waikiki, Hawaii, Oct. 28-Nov. 3, 2007.
[22] J. Uher, F. Frojdh, J. Jakubek, C. Kenney, Z. Kohout, V. Linhart, S. Parker, S. Petersson, S. Pospisil, G. Thungstrom, "Characterization of 3D Thermal Neutron Semiconductor Detectors," Nucl. Instr. Meth. A576 (2007) 32.
[23] J.K. Shultis and D.S. McGregor, "Designs for Micro-Structured Semiconductor Neutron Detectors," Proc. SPIE, Vol. 7079 (2008) pp. 06:1-06:15.
[24] N. LiCausi, J. Dingley, Y. Danon, J-Q Lu, I. B. Bhat, "A Novel Solid-State Self Powered Neuron Detector," Proc. SPIE, Vol. 7079 (2008) pp. 08:1-08:12.
[25] D.S. McGregor, S.L. Bellinger, W.J. McNeil, T.C. Unruh, "Micro-Structured High-Efficiency Semiconductor Neutron Detectors," IEEE Nuclear Science Symposium, Dresden, Germany, Oct. 19-Oct. 25, 2008.
[26] R.J. Nikolic, A.M. Conway, C.E. Reinhardt, R.T. Graff, T.F. Wang, N. Deo, C.L. Cheung, "6:1 Aspect Ratio Silicon Pillar Based Thermal Neutron Detector Filled with ^{10}B," Appl. Phys. Lett. 93 (2008) 133502.
[27] A.M. Conway, T.F. Wang, N. Deo, C.L. Cheung, R.J. Nikolic, "Numerical Simluations of Pillar Structured Solid State Thermal Neutron Detector: Efficiency and Gamma Discrimination," IEEE Trans. Nucl. Sci., NS-56 (2009) 2802.
[28] D.S. McGregor, S. Bellinger, D. Bruno, W.L. Dunn, W.J. McNeil, E. Patterson, B.B. Rice, J.K. Shultis, T. Unruh, "Perforated Diode Neutron Detector Modules Fabricated from High-Purity Silicon," Radiation Physics and Chemistry, **78** (2009) pp. 874-881.
[29] S.L. Bellinger, W.J. McNeil, D.S. McGregor, "Variant Designs and Characteristics of Improved Microstructured Solid-State Neutron Detectors," IEEE Nuclear Science Symposium, Orlando, Florida, Oct. 25-Oct. 31, 2009, pp. 986-989.
[30] W.J. McNeil, S.L. Bellinger, T.C. Unruh, C.M. Henderson, P.B. Ugorowski, W.L. Dunn, R.D. Taylor, B.J. Blalock, C.L. Britton, D.S. McGregor, "1024-Channel Solid State 1-D Pixel Array for Small Angle Neutron Scattering," IEEE Nuclear Science Symposium, Orlando, Florida, Oct. 25-Oct. 31, 2009, pp. 2008-2011.
[31] W.J. McNeil, S.L. Bellinger, T.C. Unruh, C.M. Henderson, P. Ugorowski, B. Morris-Lee, R.D. Taylor, D.S. McGregor, "1-D Array of Perforated Diode Neutron Detectors," Nucl. Instrum. Meth., **A604** (2009) pp. 127-129.

Downloaded from SPIE Digital Library on 18 Nov 2010 to 129.130.37.22. Terms of Use: http://spiedl.org/terms

[32] S.L. Bellinger, W.J. McNeil, T.C. Unruh, D.S. McGregor, "Characteristics of 3D Micro-Structured Semiconductor High Efficiency Neutron Detectors," IEEE Trans. Nucl. Sci., **NS-56** (2009) pp. 742 - 746.
[33] J.K. Shultis and D.S. McGregor, "Design and Performance Considerations for Perforated Semiconductor Thermal-Neutron Detectors," Nuclear Instruments and Methods, **A606** (2009) pp. 608-636.
[34] D.S. McGregor, W.J. McNeil, S.L. Bellinger, T.C. Unruh, J.K. Shultis, "Microstructured Semiconductor Neutron Detectors," Nucl. Instrum. and Meth. **A608** (2009) pp. 125-131.
[35] S.L. Bellinger, W.J. McNeil and D.S. McGregor, "Improved Fabrication Technique for Microstructured Solid-State Neutron Detectors," Proc. MRS, **vol. 1164** (2009) L06-01.
[36] C.M. Henderson, Q.M. Jahan, W.L. Dunn, J.K. Shultis and D.S. McGregor, "Characterization of Prototype Perforated Semiconductor Neutron Detectors," Radiation Physics and Chemistry, **79** (2010) pp. 144-150.
[37] S.L. Bellinger, R.F. Fronk, W.J. McNeil, T.J. Sobering, D.S. McGregor, Nucl. Instr. and Meth. (2010) in press.
[38] C.J. Solomon, J.K. Shultis, D.S. McGregor, "Reduced Efficiency Variation in Perforated Neutron Detectors with Sinusoidal Trench Design," Nucl. Instrum. and Meth., **A618** (2010) pp. 260-265.
[39] D.S. McGregor, R.A. Rojeski, G.F. Knoll, F.L. Terry, Jr., J. East, and Y. Eisen, "Evidence for Field Enhanced Electron Capture by EL2 Centers in Semi-Insulating GaAs and the Effect on GaAs Radiation Detectors," J. Applied Physics, 75 (1994) pp. 7910-7915; errata J. Applied Physics, **77** (1995) p. 1331.
[40] S. Wolf and R.N. Tauber, Silicon Processing for the VLSI Era, Vol. 1. Process Technology, (Lattice Press, Sunset Beach, 1986).
[41] K. E. Bean, "Anisotropic Etching of Silicon," IEEE Trans. Elect. Dev., ED-25 (1978) 1185-1193.
[42] V. McLane, C.L. Dunford, P.F. Rose, Neutron Cross Sections, Vol. 2 (Academic Press, Bonston, 1988).
[43] T.C. Unruh, "Development of a neutron diffraction system and neutron imaging system for beamport characterization," Kansas State University, Manhattan, Thesis 2009.

Downloaded from SPIE Digital Library on 18 Nov 2010 to 129.130.37.22. Terms of Use: http://spiedl.org/terms